

RESEARCH ARTICLE

An adaptive optimized Nyström method for second-order IVPs

Mufutau Ajani Rufai¹ | Francesca Mazzia² | Higinio Ramos^{3,4}

¹Dipartimento di Matematica, Università Degli Studi di Bari Aldo Moro, Bari, 70125, Italy

²Dipartimento di Informatica, Università Degli Studi di Bari Aldo Moro, Bari, 70125, Italy

³Scientific Computing Group, Universidad de Salamanca, Plaza de la Merced, Salamanca, 37008, Spain

⁴Escuela Politécnica Superior de Zamora, Campus Viriato, Zamora, 49022, Spain

Correspondence

Mufutau Ajani Rufai, Dipartimento di Matematica, Università Degli Studi di Bari Aldo Moro, Bari 70125, Italy.
Email: mufutau.rufai@uniba.it

Communicated by: T. Monovasilis

This research work deals with the development, analysis, and implementation of an adaptive optimized one-step Nyström method for solving second-order initial value problems of ODEs and time-dependent partial differential equations. The new method is developed through a collocation technique with a new approach for selecting the collocation points. An embedding-like procedure is used to estimate the error of the proposed optimized method. The current approach has been used to compute efficiently approximate solutions to general second-order IVPs. The numerical experiments demonstrate that the introduced error estimation and step-size control strategy presented in this manuscript have produced a good performance compared to some of the other existing numerical methods.

KEYWORDS

collocation method, error estimation and control, ordinary and time-dependent partial differential equations, optimized Nyström method, variable stepsize formulation

MSC CLASSIFICATION

65L05, 65L20

1 | INTRODUCTION

Second-order ordinary differential equations (ODEs) are widely used to model real-world problems in engineering, control theory, physics, economics, and social sciences, etc. In this article, we consider problems of the form

$$\begin{aligned} y''(x) &= f(x, y(x), y'(x)), \\ y(a) &= y_0, y'(a) = y'_0, x \in [a, b] \subset \mathbb{R}, y, f \in \mathbb{R}^d, \end{aligned} \quad (1)$$

where $a = x_0$ stands for the initial point; b, y_0, y'_0 are given; and f is assumed to be a continuous function that fulfills the Lipschitz's condition that guarantees the existence and uniqueness theorem in Henrici.¹ It is noteworthy to mention that a van der Pol, Kepler's, Bessel, highly stiff oscillatory, simple harmonic and critically damped motion, and other similar problems can be written in the form of (1).

Many existing numerical methods for solving the class of problem in (1) have been developed; see, for example, previous studies.^{2–12} Those strategies include Runge-Kutta type, linear multistep, Numerov-type, P-stable Obrechhoff, or collocation methods. One standard approach is to transform problem (1) into an equivalent system of first-order ODEs. Then, the resulting system of equations is solved using suitable methods for first-order ODEs (see Lambert¹³ and Hairer & Wanner¹⁴).

In order to enhance the previously mentioned techniques, scholars like Kalogiratou et al.,¹⁵ Ramos and Rufai,^{16–21} Amodio and Brugnano,²² and Rufai²³ have derived and implemented block methods for solving the class of problems in (1) directly. The advantage of block methods over the Runge-Kutta type and predictor-corrector methods is that they can be less expensive regarding the number of functions evaluated and CPU time.

Nyström methods²⁴ are a general class of methods that has been proved to be particularly effective for the special type of differential problems when the function f in (1) does not depend on $y'(x)$.^{24–26}

In this paper, we introduce a new optimized Nyström method (ONM) coupled with an associated embedded method for error estimation, which makes it suitable for a variable stepsize implementation. The obtained adaptive form of the ONM is applied to directly solve problems of type in (1), and its special form in which the function f does not depend on $y'(x)$.

2 | DERIVATION OF THE METHOD

Let $h > 0$ be the integration stepsize and $x_1 = x_0 + h$. Following the approaches in van der Houwen et al.²⁵ and Rufai and Ramos,²⁷ we assume that the exact solution of the IVP in (1) on $[x_0, x_1]$ is approximated by a polynomial $u(x_0 + sh)$, $s \in [0, 1]$ of degree 7, satisfying the collocation conditions $u''(x_{c_j}) = f_{c_j}$, where $c_0 = 0 < c_1 < c_2 < c_3 < c_4 < c_5 = 1$, $x_{c_j} = x_0 + c_j h$, $j = 1(1)4$, and $f_{c_j} = f(x_{c_j}, u(x_{c_j}), u'(x_{c_j}))$. In terms of the Lagrange basis polynomials $L_j(s)$ defined on the values $x_0 + c_j h$, $j = 0, \dots, 5$, $u''(x_0 + sh)$ reads

$$u''(x_0 + sh) = \sum_{j=0}^5 f_{c_j} L_j(s). \quad (2)$$

Integrating (2) once and twice, respectively, and exploiting the initial conditions for $s = 0$ leads to the following formulas

$$h y'(x_0 + sh) \simeq h u'(x_0 + sh) = h y'_0 + h^2 \sum_{j=0}^5 \beta_j(s) f_{c_j}, \quad (3)$$

$$y(x_0 + sh) \simeq u(x_0 + sh) = y_0 + s h y'_0 + h^2 \sum_{j=0}^5 \alpha_j(s) f_{c_j}, \quad (4)$$

where $\alpha_j(s) = \int_0^s (s-r) L_j(r) dr$ and $\beta_j(s) = \int_0^s L_j(r) dr$. We then set $y_1 = u(x_0 + h)$, $y'_1 = u'(x_0 + h)$ and iterate the above procedure on subintervals $[x_n, x_{n+1}]$, $n = 0, 1, \dots, N-1$, of length h , with $x_N = b$.

The proposed method is constructed by considering four intermediate points on $[x_0, x_1]$. A common procedure to increase the order of a collocation method is to choose the intermediate points in order to have a truncation error of higher order at the point x_1 . Here, instead of looking for the higher possible truncation error, we choose the intermediate points in order to rise by one the order of the local truncation errors for $y(x_1)$, $y'(x_1)$, and $y(x_{c_3})$. For simplicity, we fixed $c_2 = \frac{1}{2}$, and we look for the values of c_1, c_3, c_4 . The truncation errors are obtained through the expansion in powers of h utilizing the Taylor series, resulting in

$$\begin{aligned} \mathcal{L}[y(x_1), h] &= \frac{(-7c_1 c_3 c_4 + c_1 + c_3 + c_4 - 1) h^8 y^{(8)}(x_0)}{604800} + \mathcal{O}(h^9), \\ \mathcal{L}[y(x_{c_3}), h] &= \frac{h^8 y^{(8)}(x_0) P_{c_3}}{604800} + \mathcal{O}(h^9), \\ \mathcal{L}[y'(x_1), h] &= \frac{(-6 - 7c_3(-1 + c_4) + 7c_4 - 7c_1(-1 + c_3 + c_4)) h^7 y^{(8)}(x_0)}{604800} + \mathcal{O}(h^8), \end{aligned} \quad (5)$$

with

$$P_{c_3} = c_3^4 (c_3 (-5c_3^3 + (8c_4 + 12) c_3^2 - (21c_4 + 7) c_3 + 14c_4) + c_1 (8c_3^3 - (14c_4 + 21) c_3^2 + (42c_4 + 14) c_3 - 35c_4)).$$

Equating the principal terms in (5) to zero, we have

$$\begin{cases} -7c_1 c_3 c_4 + c_1 + c_3 + c_4 - 1 = 0 \\ P_{c_3} = 0 \\ -6 - 7c_3(-1 + c_4) + 7c_4 - 7c_1(-1 + c_3 + c_4) = 0. \end{cases} \quad (6)$$

After solving this system, the optimal coefficients derived by this procedure satisfying $0 < c_1 < c_3 < c_4 < 1$ are

$$c_1 = \frac{(7 - \sqrt{21})}{14}, \quad c_3 = \frac{(7 + \sqrt{21})}{14}, \quad c_4 = \frac{21 + 4\sqrt{21}}{42}.$$

Substituting the values of the coefficients and evaluating the formulas in (3) and (4) at $s = 1$, we get approximations of $y(x_0 + h)$ and $y'(x_0 + h)$, given as follows:

$$\begin{aligned} y_1 &= y_0 + hy'_0 + \frac{1}{360}h^2 \left(18f_0 + 7(\sqrt{21} + 7)f_{c_1} + 64f_{c_2} - 7(\sqrt{21} - 7)f_{c_3} \right), \\ hy'_1 &= hy'_0 + \frac{1}{180}h^2 (9f_0 + 49f_{c_1} + 64f_{c_2} + 49f_{c_3} + 9f_1). \end{aligned} \quad (7)$$

In order to implement the proposed optimized Nyström method in block form, some additional formulas must be considered. To do this, we take the values of $u(x_0 + sh)$ in (3) and $hu'(x_0 + sh)$ in (4) evaluated at the collocation points obtained for $s = c_1, c_2, c_3, c_4$. In this way, we obtain a total of 10 formulas that form the proposed optimized Nyström method.

3 | THEORETICAL ANALYSIS

The obtained ONM can be formulated in matrix form as

$$\bar{R}V_0 = h\bar{S}V'_0 + h^2\bar{T}F_0, \quad (8)$$

with $\bar{R}, \bar{S}, \bar{T}$ constant matrices containing the coefficients of the ONM, given by

$$\bar{R} = \begin{pmatrix} -1 & 1 & 0 & 0 & 0 & 0 \\ -1 & 0 & 1 & 0 & 0 & 0 \\ -1 & 0 & 0 & 1 & 0 & 0 \\ -1 & 0 & 0 & 0 & 1 & 0 \\ -1 & 0 & 0 & 0 & 0 & 1 \\ 0 & 0 & 0 & 0 & 0 & 0 \\ 0 & 0 & 0 & 0 & 0 & 0 \\ 0 & 0 & 0 & 0 & 0 & 0 \\ 0 & 0 & 0 & 0 & 0 & 0 \\ 0 & 0 & 0 & 0 & 0 & 0 \end{pmatrix}; \quad \bar{S} = \begin{pmatrix} \frac{1}{14}(7 - \sqrt{21}) & 0 & 0 & 0 & 0 & 0 \\ \frac{1}{2} & 0 & 0 & 0 & 0 & 0 \\ \frac{1}{14}(\sqrt{21} + 7) & 0 & 0 & 0 & 0 & 0 \\ \frac{1}{2} + \frac{2}{\sqrt{21}} & 0 & 0 & 0 & 0 & 0 \\ 1 & 0 & 0 & 0 & 0 & 0 \\ 1 & -1 & 0 & 0 & 0 & 0 \\ 1 & 0 & -1 & 0 & 0 & 0 \\ 1 & 0 & 0 & -1 & 0 & 0 \\ 1 & 0 & 0 & 0 & -1 & 0 \\ 1 & 0 & 0 & 0 & 0 & -1 \end{pmatrix}; \quad (9)$$

$$\bar{T} = \begin{pmatrix} \frac{1111-171\sqrt{21}}{41160} & \frac{55}{6174} & \frac{2(419-98\sqrt{21})}{15435} & \frac{1709-343\sqrt{21}}{17640} & -\frac{18}{1715} & \frac{12\sqrt{21}+41}{20580} \\ \frac{49}{1920} & \frac{7(8\sqrt{21}+35)}{5760} & \frac{1}{72} & -\frac{7(8\sqrt{21}-35)}{5760} & 0 & \frac{1}{1920} \\ \frac{171\sqrt{21}+919}{41160} & \frac{2401\sqrt{21}+11003}{123480} & \frac{2(98\sqrt{21}+449)}{15435} & \frac{1}{882} & \frac{18}{1715} & \frac{-12\sqrt{21}-55}{20580} \\ \frac{88612\sqrt{21}+426493}{17781120} & \frac{49\sqrt{\frac{7}{3}}}{720} + \frac{5545181}{53343360} & \frac{129361}{1666980} + \frac{16}{45\sqrt{21}} & \frac{7\sqrt{\frac{7}{3}}}{720} + \frac{112019}{7620480} & \frac{25}{24696} & \frac{-788\sqrt{21}-3607}{3556224} \\ \frac{1}{20} & \frac{7}{360}(\sqrt{21} + 7) & \frac{8}{45} & \frac{1}{360}(-7)(\sqrt{21} - 7) & 0 & 0 \\ \frac{41\sqrt{21}+189}{5880} & \frac{49}{360} - \frac{23}{840\sqrt{21}} & \frac{8}{45} - \frac{106}{105\sqrt{21}} & \frac{343-29\sqrt{21}}{2520} & -\frac{1}{35}\left(6\sqrt{\frac{3}{7}}\right) & \frac{1}{56} + \frac{41}{280\sqrt{21}} \\ \frac{1}{960}(81 - 8\sqrt{21}) & \frac{95\sqrt{21}+392}{2880} & \frac{\sqrt{\frac{7}{3}}}{48} + \frac{8}{45} & -\frac{7(25\sqrt{21}-56)}{2880} & \frac{3\sqrt{21}}{80} & \frac{1}{960}(-8\sqrt{21} - 33) \\ \frac{23\sqrt{21}+189}{5880} & \frac{49}{360} + \frac{523}{840\sqrt{21}} & \frac{8}{45} + \frac{86}{105\sqrt{21}} & \frac{7}{360}(\sqrt{21} + 7) & -\frac{1}{35}\left(6\sqrt{\frac{3}{7}}\right) & \frac{1}{56} + \frac{23}{280\sqrt{21}} \\ \frac{3368\sqrt{21}+48027}{1270080} & \frac{49}{360} + \frac{113269}{181440\sqrt{21}} & \frac{8}{45} + \frac{36871}{45360\sqrt{21}} & \frac{49}{360} + \frac{16717}{25920\sqrt{21}} & -\frac{65}{336\sqrt{21}} & \frac{737}{60480} + \frac{421}{7560\sqrt{21}} \\ \frac{1}{20} & \frac{49}{180} & \frac{16}{45} & \frac{49}{180} & 0 & \frac{1}{20} \end{pmatrix}, \quad (10)$$

and

$$\begin{aligned} V_0 &= (y_0, y_{c_1}, y_{c_2}, y_{c_3}, y_{c_4}, y_1)^\top, \\ V'_0 &= (y'_0, y'_{c_1}, y'_{c_2}, y'_{c_3}, y'_{c_4}, y'_1)^\top, \\ F_0 &= (f_0, f_{c_1}, f_{c_2}, f_{c_3}, f_{c_4}, f_1)^\top. \end{aligned}$$

We define the operator Γ related to the ONM in (8), assuming that $y(x)$ has enough derivatives, as

$$\Gamma[y(x); h] = \sum_{j \in I} [\theta_j y(x + jh) - h\Theta_j y'(x + jh) - h^2\vartheta_j y''(x + jh)], \quad (11)$$

where θ_j , Θ_j , and ϑ_j are, respectively, vector columns of \bar{R} , \bar{S} , and \bar{T} , and $I = \{0, c_1, c_2, c_3, c_4, 1\}$.

Expanding $y(x_0 + jh)$, $y'(x_0 + jh)$, and $y''(x_0 + jh)$ in Taylor series about x_0 , we have

$$\Gamma[y(x); h] = C_0 y(x) + C_1 h y'(x) + C_2 h^2 y''(x) + \dots + C_q h^q y^{(q)}(x) + \dots, \quad (12)$$

where

$$C_q = \frac{1}{q!} \left[\sum_{j \in I} j^q \theta_j - q \sum_{j \in I} j^{q-1} \Theta_j - q(q-1) \sum_{j \in I} j^{q-2} \vartheta_j \right], \quad (13)$$

and $q = 0, 1, 2, 3, 4, \dots$. The order of the local truncation error is determined by the first non-null vector C_q .

We note that the resulting scheme is a Nyström method based on direct collocation. According to van der Houwen et al.,²⁵ if

$$y(x_1) - y_1 = O(h^{p_1+1}), \quad y'(x_1) - y'_1 = O(h^{p_2+1}),$$

then the order of accuracy is defined as $p = \min\{p_1, p_2\}$.

By van der Houwen et al.,^{25, theorem 3.2} we know that the method has global step point order of at least $p = 6$, and locally, the order of the y component is 7, and the order of the y' component is one lower. We have increased the global step point order with the special choice of the collocation points. Since van der Houwen et al.^{25, theorem 3.4} is satisfied with $p = s + q = 6 + 2 = 8$, then the ONM has global step point order $p = 8$.

By substituting the elements of the matrices defined in (9) and (10), we get the orders and LTEs for each of the formulas in (8), as given in Table 1.

The proposed method can be simplified for special differential equations, obtaining a class of Runge-Kutta-Nyström methods. To study the stability properties, we consider two test equations, and the first one is the standard one for special equations:

$$y''(x) = -\nu^2 y(x), \quad \nu > 0. \quad (14)$$

TABLE 1 Order(p) and local truncation errors (LTEs) for the formulas in (8)

Formula	Order	Local truncation errors
y_{c_1}	7	$-\frac{h^8 y^{(8)}(x_0)}{36303120} + \mathcal{O}(h^9)$
y_{c_2}	7	$-\frac{h^8 y^{(8)}(x_0)}{30965760} + \mathcal{O}(h^9)$
y_{c_3}	7	$\frac{(523\sqrt{21}+2401)h^9 y^{(9)}(x_0)}{853849382400} + \mathcal{O}(h^{10})$
y_{c_4}	7	$-\frac{125h^8 y^{(8)}(x_0)}{1204450394112} + \mathcal{O}(h^9)$
y_1	8	$\frac{h^9 y^{(9)}(x_0)}{177811200} + \mathcal{O}(h^{10})$
y'_{c_1}	6	$-\frac{11h^7 y^{(8)}(x_0)}{8297856\sqrt{21}} + \mathcal{O}(h^8)$
y'_{c_2}	6	$\frac{h^7 y^{(8)}(x_0)}{967680\sqrt{21}} + \mathcal{O}(h^8)$
y'_{c_3}	6	$-\frac{h^7 y^{(8)}(x_0)}{41489280\sqrt{21}} + \mathcal{O}(h^8)$
y'_{c_4}	6	$\frac{25h^7 y^{(8)}(x_0)}{1792336896\sqrt{21}} + \mathcal{O}(h^8)$
y'_1	8	$-\frac{h^9 y^{(10)}(x_0)}{1422489600} + \mathcal{O}(h^{10})$

The second one is defined for general problems:

$$y''(x) = -2\nu y'(x) - \nu^2 y(x), \quad \nu > 0. \quad (15)$$

The above equations have bounded solutions that go to zero as x tends to infinity. Applying the ONM in (8) on (14) and (15), we have

$$P \begin{pmatrix} y_{c_1} \\ y_{c_2} \\ y_{c_3} \\ y_{c_4} \\ y_1 \\ y'_{c_1} \\ y'_{c_2} \\ y'_{c_3} \\ y'_{c_4} \\ y'_1 \end{pmatrix} = Q \begin{pmatrix} y_{c_1-1} \\ y_{c_2-1} \\ y_{c_3-1} \\ y_{c_4-1} \\ y_0 \\ y'_{c_1-1} \\ y'_{c_2-1} \\ y'_{c_3-1} \\ y'_{c_4-1} \\ y'_0 \end{pmatrix},$$

where P and Q are square matrices of dimension 10 whose entries are obtained from the coefficients of the formulas given in (8). By letting $z = \nu h$, we study the stability of the proposed ONM through the eigenvalues of the amplification matrix ($M(z) = P^{-1}Q$).

Definition 3.1. (Atkinson²⁸) The region of absolute stability of a numerical method is the set of all values νh , considered as a subset of the complex plane, for which $y_n \rightarrow 0$ as $h \rightarrow 0$.

Figures 1 and 2 display the stability regions of the proposed ONM using the above test equations.

4 | ERROR ESTIMATION AND MESH SELECTION

From a practical point of view, it might be unreasonable to solve an IVP with a constant stepsize, especially when the true solution changes at very different rates in different parts of the integration interval $[x_0, x_N]$. Thus, for the numerical method (8) to be reliable and, of course, efficient, it must be suitable for a variable stepsize (VSS) implementation. The approach of VSS is also known as adaptive since it adjusts the number and position of the steps utilized in the numerical solution to ensure that the truncation error is kept below a predefined tolerance. To achieve a robust estimation of the local truncation error (LTE), we adopted a similar strategy as in Shampine and Gordon.²⁹

Choosing a higher order formula that could be used for error estimation is not so simple. We use a strategy that requires two more function evaluations. Following the procedure described in Iavernaro and Mazzia,³⁰ but starting from the Hermite-Obreschkoff methods presented in Mazzia and Sestini,³¹ we use a central finite difference approach to get the coefficients for computing an approximation y_1^* to $y(x_1)$. The derivatives of the Hermite-Obreschkoff method of order 10 are approximated using a stencil of eight points with the previous computed function values f_{c_i} , $i = 0, \dots, 5$ and two additional function evaluations at the points $c_6 = \frac{1}{2} - \frac{2}{\sqrt{21}}$ and $c_7 = \frac{3}{2} - \frac{2}{\sqrt{21}}$. The approximations of y_{c_j} , y'_{c_j} , $j = 6, 7$ needed

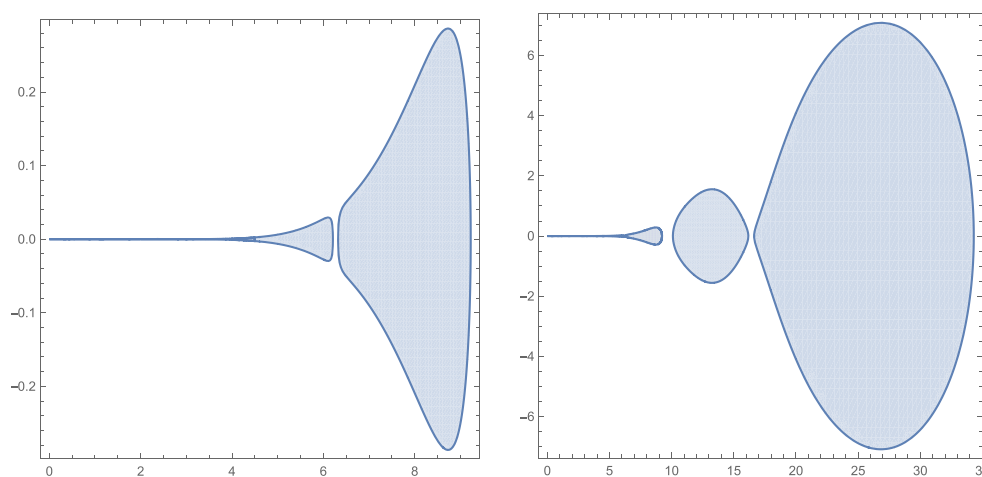
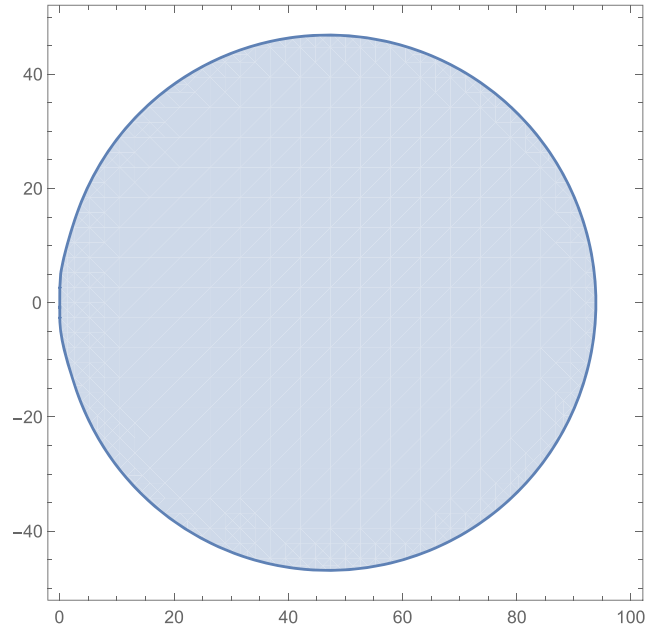


FIGURE 1 Stability region in the complex z plane using (14) [Colour figure can be viewed at wileyonlinelibrary.com]

FIGURE 2 Stability region in the complex z plane using (15)
[Colour figure can be viewed at wileyonlinelibrary.com]



for the evaluation of f are computed through the collocation polynomial, requiring a linear combination of the function values. The following multistep formula of order $p = 8$ is then obtained:

$$\begin{aligned}
 y_1^* = y_0 + hy_0' + h^2 & \left(\frac{(2343 - 16\sqrt{21})f_0}{51900} - \frac{(4\sqrt{21} + 21)f_1}{375} + \frac{(573\sqrt{21} + 3731)f_{c_1}}{29880} \right) \\
 & + h^2 \left(\frac{(2\sqrt{21} + 565)f_{c_2}}{3060} + \frac{(197 - 43\sqrt{21})f_{c_3}}{1800} \right) \\
 & + h^2 \left(\frac{3(4\sqrt{21} + 21)f_{c_4}}{1000} + \frac{3f_{c_6}}{200} + \frac{3(30854\sqrt{21} + 141421)f_{c_7}}{30512875} \right), \quad (16)
 \end{aligned}$$

with local truncation error $LTE = \frac{4\sqrt{21}-63}{59744563200}h^{10}y^{(10)}(x_0) + O(h^{11})$.

We need an error estimate that provides the basis for choosing the stepsize for the next step. The mesh selection is made by computing an estimation of the relative mixed error as follows:

$$EST = \frac{\|y_1^* - y_1\|}{\left(\frac{ATOL}{RTOL} + \|y_1\|\right)},$$

where y_1^* and y_1 are the values obtained by the formula in (16) and the method in (8), respectively, and ATOL and RTOL are the user's predefined tolerances. Let us define

$$\delta = \mu \times \left(\frac{RTOL}{EST} \right)^{1/p},$$

where according to Stoer and Bulirsch,^{32, p. 491} $0 < \mu < 1$ is a suitable adjustment factor to avoid rejected steps.

If $EST \leq RTOL$, then we accept the results and take the next step as

$$h_{new} = \min \{ 10 \times h_{old}, \delta \times h_{old} \};$$

that is, we proceed with the integration limiting the new stepsize to a maximum of $10 \times h_{old}$. On the other hand, if $EST > RTOL$, then we reject the obtained results and repeat the calculations with the following new step:

$$h_{new} = \max \{ 10^{-1} \times h_{old}, \delta \times h_{old} \}. \quad (17)$$

In the numerical experiments section, we have used $\mu = 0.95$. Furthermore, we have provided values such that $h_{min} \leq h_{new} \leq h_{max}$, where h_{min} and h_{max} are the minimum and maximum stepsizes allowed, respectively.

For comparison purposes, the implicit Lobatto III-A Runge-Kutta method of order 8 has been implemented as an embedded Runge-Kutta method in variable stepsize mode. The following multistep formula of order $p = 10$

$$y_1^* = y_0 + \frac{h \left(182475f_0 + 2064384f_{\frac{1}{4}} + 2064384f_{\frac{3}{4}} + 2097152f_{\frac{5}{8}} + 2097152f_{\frac{7}{8}} \right)}{5953500} + \frac{h \left(-2067261f_{c_1} + 1400000f_{c_2} - 2067261f_{c_3} + 182475f_1 \right)}{5953500}, \quad (18)$$

with local truncation error $LTE = -\frac{17}{90128941056000}h^{11}y^{(11)}(x_0) + O(h^{12})$ has been used to estimate the local error at each step and a similar strategy for mesh selection as given above with $p = 10$ has also been utilized with the Runge-Kutta method.

5 | COMPUTATIONAL DETAILS

The new ONM is implemented in a step by step mode. We denote the obtained system from (8) as $\mathbf{F}(\mathbf{y}) = \mathbf{0}$ where the unknowns are

$$\tilde{\mathbf{Y}} = (y_{c_1}, y'_{c_1}, y_{c_2}, y'_{c_2}, y_{c_3}, y'_{c_3}, y_{c_4}, y'_{c_4}, y_1, y'_1).$$

Since the ONM is an implicit scheme, we use a Modified Newton's method (MNM) to solve the obtained systems. The i th iteration of the MNM is given by

$$\mathbf{J}_0^i (\tilde{\mathbf{Y}}^{i+1} - \tilde{\mathbf{Y}}^i) = -\mathbf{F}^i,$$

where \mathbf{J}_0^i represents the frozen jacobian matrix of \mathbf{F} at the starting value. The starting values to be used by MNM for solving the system on each iteration are taken as

$$y_{n+j} = y_n + (jh)y'_n + \frac{(jh)^2}{2}f_n, \quad y'_{n+j} = y'_n + (jh)f_n, \quad n = 0, 1, 2, \dots, N-1, \quad j = c_1, c_2, c_3, c_4, 1.$$

We can apply the ONM to solve systems of second-order IVPs by considering the following system of m equations:

$$\mathbf{y}'' = \mathbf{f}(x, \mathbf{y}^\top, \mathbf{y}'^\top), \quad \mathbf{y}(a) = \mathbf{y}_0, \quad \mathbf{y}'(a) = \dot{\mathbf{y}}_0, \quad a = x_0 \leq x \leq b = x_N,$$

where $\mathbf{y} = (y_1, \dots, y_d)^\top, \mathbf{y}' = (y'_1, \dots, y'_d)^\top,$

$$\mathbf{f}(x, \mathbf{y}^\top, \mathbf{y}'^\top) = (f_1(x, \mathbf{y}^\top, \mathbf{y}'^\top), \dots, f_d(x, \mathbf{y}^\top, \mathbf{y}'^\top))^\top,$$

and $\mathbf{y}_0 = (y_{1,0}, \dots, y_{d,0})^\top, \dot{\mathbf{y}}_0 = (\dot{y}_{1,0}, \dots, \dot{y}_{d,0})^\top$. In the case of d -dimensional IVPs, we get an algebraic system of $10d$ equations, and we solved the resulting non-linear system using MNM, as in the case of scalar one-dimensional IVPs. The stopping criterion and the maximum number of iterations used while executing the MNM are $2 \times RTOL$ and 100, respectively.

6 | NUMERICAL EXPERIMENTS

Here, we report the numerical performance of the proposed ONM on the class of second-order problems of the form (1). We note that the effectiveness and efficiency of the proposed strategy rely on the method itself, but also in the VSS technique presented in Section 4. The criteria utilized as a measure of the accuracy are the maximum absolute error (MAE) and the maximum relative error (MRE) on the integration interval, given, respectively, by the formulas

$$MAE = \max_{j=0, \dots, N} \{ \|y(x_j) - y_j\|_\infty \},$$

$$MRE = \max_{j=0, \dots, N} \left\{ \frac{\|y(x_j) - y_j\|}{\left(\frac{ATOL}{RTOL} + \|y(x_j)\| \right)} \right\},$$

where $y(x_j)$ is the exact solution and y_j is the computed result at each point x_j of the discrete grid.

To measure the computational order of convergence, we use the common formula

$$ROC = -\log_2 \left(\frac{MAE_h}{MAE_{2h}} \right).$$

The following abbreviations are utilized in the tables:

- ONM: The new optimized Nyström method developed in this paper.
- FM8P: The Falkner method of order eight (see Vigo-Aguiar & Ramos³³).
- FDM8P: The finite difference method of order eight (see Amodio et al.^{34,35}).
- FDM9P-GFD: The finite difference method of order nine with generalized backward difference (see Amodio et al.^{34,35}).
- FDM9P-GBD: The finite difference method of order nine with generalized forward difference (see Amodio et al.^{34,35}).
- LOB-III A8P: The implicit Lobatto III-A Runge-Kutta method of order eight formulated in variable stepsize using the multistep formula of order ten in (18) (see Butcher³⁶).
- ERKNM: The embedded Runge-Kutta-Nyström method in Dormand et al.³⁷
- NS: Number of steps.
- NA: Not applicable.
- NRS: Number of rejected steps.
- NNI: Number of Newton iterations.
- NJ: Number of Jacobian evaluations.
- ABE $y(x)$: Absolute error of the solution.
- ABE $y'(x)$: Absolute error of the first derivative solution.
- TFE: Total number of function evaluations.
- h_{ini} : Initial stepsize.
- h_{min} : Minimum stepsize allowed.
- h_{max} : Maximum stepsize allowed.
- ATOL: Absolute Tolerance.
- RTOL: Relative Tolerance.
- CPU: Computational time in seconds.

6.1 | Numerical experiment 1

To determine the numerical rate of convergence of the proposed ONM, we first consider the following Bessel problem using fixed stepsize:

$$x^2 y''(x) + x y'(x) + (x^2 - 0.25) y(x) = 0,$$

$$y(1) = \sqrt{\frac{2}{\pi}} \sin(1), \quad y'(1) = \frac{2 \cos(1) - \sin(1)}{\sqrt{2\pi}}, \quad 1 \leq x \leq 8, \quad (19)$$

whose exact solution is

$$y(x) = \sqrt{\frac{2}{\pi x}} \sin(x).$$

In Table 2, we have included the numerical rate of convergence (ROC) to (19), which confirmed the order of convergence of the proposed method. In Table 3, we present the comparison of the numerical results for (19). We observe that the proposed ONM shows a good performance.

6.2 | Numerical experiment 2

Consider the non-linear homogeneous problem³⁴

$$\begin{aligned} (y(x) + 1)y''(x) - 3(y'(x))^2 &= 0, \\ y(1) = 0, y'(1) &= -\frac{1}{2}, \quad 1 \leq x \leq 10, \end{aligned} \quad (20)$$

whose exact solution is

$$y(x) = \frac{1}{\sqrt{x}} - 1.$$

h	Method	MAE	ROC
$\frac{1}{10}$	ONM	1.88947×10^{-8}	
$\frac{1}{20}$	ONM	1.13901×10^{-10}	7.37
$\frac{1}{40}$	ONM	5.26579×10^{-13}	7.76
$\frac{1}{80}$	ONM	2.27596×10^{-15}	7.85

TABLE 2 MAEs and computational order of convergence for test problem (19)

TABLE 3 Comparison of the numerical results for Problem (19) with $h_{ini} = 10^{-1}$

ATOL = RTOL	Method	NS	NRS	NNI	TFE	NJ	CPU	MRE
10^{-6}	ONM	6	1	14	48	7	0.02771	5.17635×10^{-6}
	LOB-III A8P	6	0	12	54	7	0.05109	3.02426×10^{-5}
	FM8P	49	NA	NA	56	NA	NA	1.71104×10^{-4}
10^{-7}	ONM	7	1	16	56	8	0.02974	2.96950×10^{-7}
	LOB-III A8P	7	1	16	63	16	0.06797	1.52460×10^{-5}
	FM8P	59	NA	NA	66	NA	NA	1.11851×10^{-5}
10^{-8}	ONM	8	1	18	64	9	0.03219	8.23386×10^{-8}
	LOB-III A8P	8	0	16	72	8	0.07570	2.14284×10^{-6}
	FM8P	69	NA	NA	76	NA	NA	8.01110×10^{-6}

TABLE 4 Comparison of the numerical results for Problem (20) with $h_{ini} = 8 \times 10^{-2}$

ATOL = RTOL	Method	NS	NRS	NNI	TFE	NJ	CPU	MRE
10^{-6}	ONM	8	0	35	64	8	0.04002	9.14896×10^{-8}
	LOB-III A8P	9	0	30	81	9	0.04904	9.82088×10^{-8}
	FDM8P	6	0	68	49	40	NA	9.56000×10^{-7}
	FDM9P-GFD	5	0	34	16	11	NA	5.89000×10^{-7}
	FDM9P-GBD	5	0	34	16	11	NA	5.74000×10^{-7}
10^{-7}	ONM	9	0	41	72	9	0.04216	1.72995×10^{-8}
	LOB-III A8P	10	0	34	90	10	0.05003	2.56512×10^{-8}
	FDM8P	7	0	77	54	44	NA	1.24000×10^{-7}
	FDM9P-GFD	6	0	67	47	38	NA	8.14000×10^{-8}
	FDM9P-GBD	6	0	67	47	38	NA	7.57000×10^{-8}
10^{-8}	ONM	10	0	47	90	10	0.04660	5.07498×10^{-9}
	LOB-III A8P	11	0	38	99	11	0.05317	5.67599×10^{-9}
	FDM8P	9	0	102	71	58	NA	1.98000×10^{-8}
	FDM9P-GFD	7	0	77	53	43	NA	8.77000×10^{-9}
	FDM9P-GBD	7	0	77	53	43	NA	8.18000×10^{-9}

Table 4 presents the comparison of maximum relative errors on the integration interval and the number of steps for different methods, evincing the good performance of the proposed ONM.

6.3 | Numerical experiment 3

Consider the van der Pol problem that arises from electronics and illustrates the behavior of non-linear vacuum tube circuits³⁸

$$\begin{aligned} y''(x) &= \nu(1 - y(x)^2)y'(x) - y(x), \\ y(0) &= 2, \quad y'(0) = 0, \quad 0 \leq x \leq 2,000, \end{aligned} \quad (21)$$

whose exact solution is unknown.

In order to compare the MREs for problem (21), the following reference solution at the final point $x_N = 2,000$ given in Mazzia and Iavernaro³⁸ has been used:

$$y(x_N) = 1.706167732170469, \quad y'(x_N) = -0.0008928097010248125.$$

The comparison of the results for the proposed ONM and LOB-III A8P presented in Table 5 was obtained using $h_{min} = 10^{-14}$ and $h_{max} = 10$, respectively.

TABLE 5 Comparison of the numerical results for Problem (21) with $h_{ini} = 10^{-2}$, $\nu = 1,000$

ATOL = RTOL	Method	NS	NRS	NNI	TFE	NJ	CPU	MRE
10^{-7}	ONM	260	147	2080	1250	407	1.73495	2.55852×10^{-8}
	LOB-III A8P	722	57	1948	6498	779	2.58218	3.01167×10^{-7}
10^{-9}	ONM	272	110	2176	1186	382	1.87437	1.24051×10^{-10}
	LOB-III A8P	747	65	2550	6723	812	3.02154	3.17159×10^{-8}
10^{-11}	ONM	405	222	1904	3240	627	2.80064	3.42564×10^{-12}
	LOB-III A8P	767	122	889	6903	889	3.65093	2.31045×10^{-9}

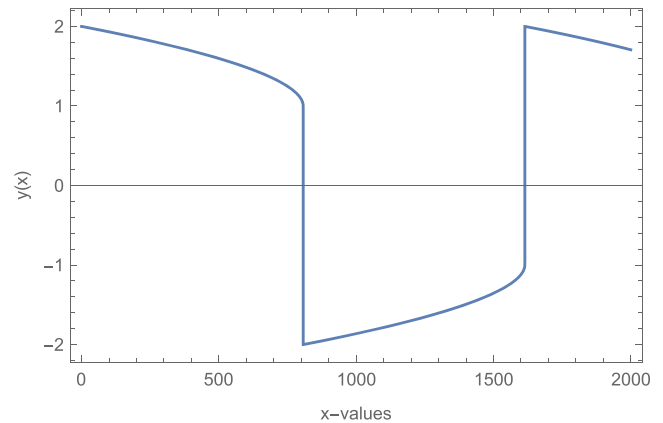


FIGURE 3 Discrete solution for (21) with $ATOL = RTOL = 10^{-9}$, $h_{ini} = 10^{-3}$ [Colour figure can be viewed at wileyonlinelibrary.com]

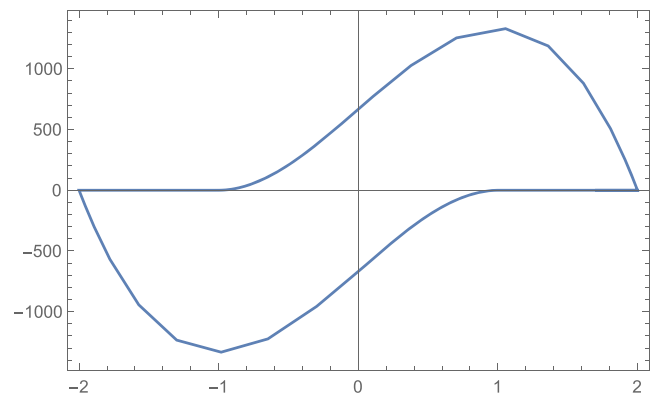


FIGURE 4 Limit cycle for the numerical experiment (21) with $ATOL = RTOL = 10^{-9}$, $h_{ini} = 10^{-3}$ [Colour figure can be viewed at wileyonlinelibrary.com]

The data in Table 5 clearly show that the best performance corresponds to the ONM. The behavior of the approximate solutions and the corresponding limit cycle are shown in Figures 3 and 4, respectively.

6.4 | Numerical experiment 4

In the fourth experiment, we solve the Kepler's problem (KP)³⁹

$$\begin{aligned} y_1''(x) &= -\frac{y_1(x)}{(y_1^2(x) + y_2^2(x))^{\frac{3}{2}}}, y_1(0) = 1 - \epsilon, y_1'(0) = 0, \\ y_2''(x) &= -\frac{y_2(x)}{(y_1^2(x) + y_2^2(x))^{\frac{3}{2}}}, y_2(0) = 0, y_2'(0) = \sqrt{\frac{1+\epsilon}{1-\epsilon}}, 0 \leq x \leq 20\pi. \end{aligned} \quad (22)$$

The theoretical solution of the KP is

$$y_1(x) = \cos(v) - \epsilon, y_2(x) = \sqrt{1 - \epsilon^2} \sin(v),$$

where v is the solution of the Kepler's equation, $v - \epsilon \sin(v) - x = 0$.

The comparison of the results for the proposed ONM, LOB-III8P, and ERKNM presented in Table 6 was obtained using $h_{min} = 10^{-14}$ and $h_{max} = 5$, respectively. The discrete solution in the phase plane is shown in Figure 5.

6.5 | Numerical experiment 5

Consider the time dependent semi-discretization of the problem given in²⁵

$$\begin{aligned} \frac{\partial^2 y}{\partial t^2} &= \frac{y^2}{(1 + 2x - 2x^2)} \frac{\partial^2 y}{\partial x^2} + y(4\cos^2(t) - 1), \\ 0 \leq t \leq 2\pi, 0 \leq x \leq 1, \end{aligned} \quad (23)$$

TABLE 6 Comparison of the numerical results for problem (22) with $h_{ini} = 10^{-2}$, $\epsilon = 0.9$

ATOL = RTOL	Method	NS	NRS	NNI	TFE	NJ	CPU	MRE
10^{-7}	ONM	267	137	1,402	2,136	404	2.62776	2.06034×10^{-2}
	LOB-III8P	278	120	1,820	2,502	398	5.49477	1.62833×10^{-2}
	ERKNM	895	351	NA	5,370	NA	0.14576	5.69382×10^{-3}
10^{-9}	ONM	379	181	1,757	3,032	560	3.50323	1.05142×10^{-4}
	LOB-III8P	420	189	2,637	3,780	609	8.16501	1.47903×10^{-4}
	ERKNM	2,107	88	NA	12,642	NA	0.27514	4.37373×10^{-6}
10^{-11}	ONM	590	280	2,611	4,720	870	5.39500	4.02528×10^{-6}
	LOB-III8P	667	288	3,938	6,003	955	12.64071	1.09840×10^{-5}
	ERKNM	5,284	3	NA	31,704	NA	0.67645	3.48023×10^{-8}

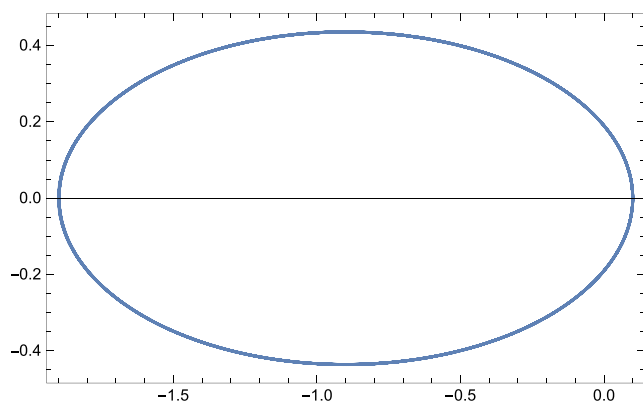
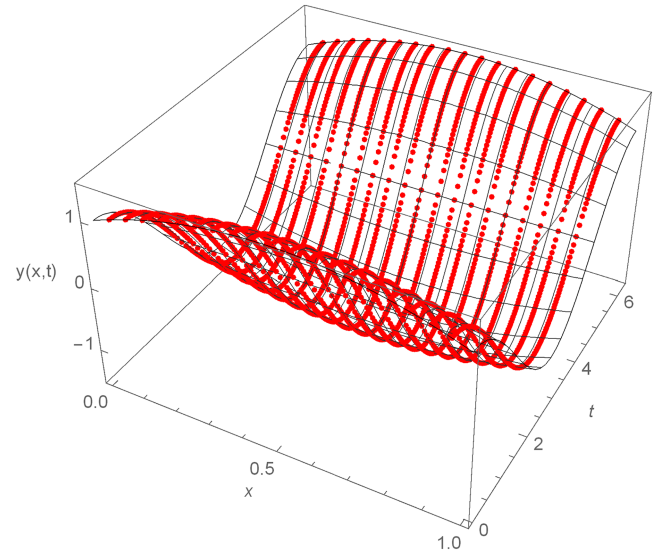


FIGURE 5 Discrete solutions for problem (22) with $ATOL = RTOL = 10^{-14}$, $h_{ini} = 10^{-2}$ [Colour figure can be viewed at wileyonlinelibrary.com]

TABLE 7 Comparison of the numerical results for Problem (23) with $h_{ini} = 10^{-2}$, $N = 19$

ATOL = RTOL	Method	NS	NRS	NNI	TFE	NJ	CPU	MRE
10^{-2}	ONM	38	20	109	304	58	20.68750	1.38480×10^{-8}
	LOB-III A8P	65	16	171	520	81	59.95313	4.38220×10^{-8}
10^{-3}	ONM	69	67	269	552	136	50.53125	8.28131×10^{-11}
	LOB-III A8P	182	15	424	1,456	197	135.09400	2.77364×10^{-11}
10^{-4}	ONM	146	150	590	1,168	296	112.78125	2.60749×10^{-14}
	LOB-III A8P	556	13	1,154	4,448	569	416,10938	$1,16304 \times 10^{-13}$

**FIGURE 6** Exact and discrete solution (red points) for (23) with $ATOL = RTOL = 10^{-4}$, $h_{ini} = 10^{-2}$ [Colour figure can be viewed at wileyonlinelibrary.com]

with initial and Dirichlet boundary conditions so that the exact solution is

$$y(x, t) = (1 + 2x - 2x^2) \cos(t).$$

We solved (23) by discretizing the second-order spatial derivative, leaving the time variable continuous, and then applying the ONM, following a procedure as in the method of lines. The $\frac{\partial^2 y}{\partial x^2}$ in (23) is discretized by

$$\frac{\partial^2 y}{\partial x^2}(x_i, t) \simeq \frac{y(x_{i+1}, t) - 2y(x_i, t) + y(x_{i-1}, t))}{\delta x^2}, \quad (24)$$

where $\delta x = \frac{(x_{N+1} - x_0)}{N+1}$, N is the internal number of spatial nodes, and $x_1 = x_0 + \delta x$, \dots , $x_N = x_0 + N\delta x$, $x_{N+1} = x_0 + (N+1)\delta x$. Taking $N = 19$ and using (24) on the grid points $x_i = \frac{i}{20}$, $i = 1, \dots, N$, we get $y_1, y_2, y_3, \dots, y_N$ by solving the following system of differential equations after replacing $\frac{\partial^2 y}{\partial x^2}(x_i, t)$ in (24) into (23),

$$y_i'' = \frac{y_i^2}{1 + 2x_i - 2x_i^2} \frac{y_{i+1} - 2y_i + y_{i-1}}{\delta x^2} + y_i(4\cos^2(t) - 1), \quad i = 1, \dots, N. \quad (25)$$

Table 7 presents the numerical results we obtained using $h_{min} = 10^{-14}$ and $h_{max} = 1$. Data in Table 7 and Figure 6 also ascertain the viability and effectiveness of the proposed ONM. Exact and approximate solutions of the ONM for (23) utilizing $h_{min} = 10^{-14}$ and $h_{max} = 1$ are plotted in Figure 6.

7 | CONCLUSIONS

A new superconvergent collocation optimized Nyström method has been developed for the solution of second-order initial value problems. In particular, an accurate way to estimate the local truncation error allow us to implement an effective

mesh selection strategy. The numerical results show that this method can be competitive with other existing numerical techniques.

ACKNOWLEDGEMENTS

The authors thank Giuseppina Settanni for providing the results of example (20) and Felice Iavernaro for useful discussions during the preparation of the paper. The first two authors are members of the INdAM Research group GNCS.

CONFLICT OF INTEREST

This work does not have any conflict of interest.

ORCID

Mufutau Ajani Rufai  <https://orcid.org/0000-0003-1293-4719>

Francesca Mazzia  <https://orcid.org/0000-0003-1072-9578>

Higinio Ramos  <https://orcid.org/0000-0003-2791-6230>

REFERENCES

1. Henrici P. Discrete variable methods in ODEs. 1962.
2. Brugnano L, Trigiante D. *Solving Differential Problems by Multistep Initial and Boundary Value Methods*: Gordon and Breach Science Publishers; 1998;280-299.
3. Simos TE, Tsitouras Ch. A new family of 7 stages, eight-order explicit Numerov-type methods. *Math Methods Appl Sci*. 2017;40(18):7876-7878.
4. Butcher JC, Hojjati G. Second derivative methods fifth Runge-Kutta stability. *Numer Algo*. 2005;40:415-429.
5. Mazzia F, Sestini A, Trigiante D. B-Spline linear multistep methods and their continuous extensions. *SIAM J Numer Anal*. 2006;44(5):1954-1973.
6. Franco J. Runge-Kutta-Nyström methods adapted to the numerical integration of perturbed oscillators. *Comput Phys Comm*. 2002;147:770-787.
7. Khalsarai MM, Shokri A. An explicit six-step singularly P-stable Obrechhoff method for the numerical solution of second-order oscillatory initial value problems. *Numer Algo*. 2020;84:871-886.
8. Mazzia F, Nagy AM. A new mesh selection strategy with stiffness detection for explicit Runge-Kutta methods. *J Appl Math Comput*. 2015;255(15):125-134.
9. Jator SN, Li J. A self starting linear multistep method for the direct solution of the general second order initial value problems. *Int J Comput Math*. 2009;86(5):817-836.
10. Berg DB, Simos TE, Tsitouras Ch. Trigonometric fitted, eight-order explicit Numerov-type methods. *Math Methods Appl Sci*. 2018;41(5):1845-1854.
11. Manni C, Mazzia F, Sestini A, Speleers H. BS2 methods for semi-linear second order boundary value problems. *J Appl Math Comput*. 2015;255:147-156.
12. You X, Zhang R, Huang T. Symmetric collocation ERKN methods for general second-order oscillators. *Calcolo*. 2019;56:52.
13. Lambert JD. *Numerical Methods for Ordinary Differential Systems*. New York: John Wiley; 1991.
14. Hairer E, Wanner G. *Solving ordinary differential equations II, stiff and differential-algebraic problems*. Second Revised Edition. *Springer-Series Comput Math*. 1996;14:75-77.
15. Ramos H, Kalogiratou Z, Monovasilis Th, Simos TE. An optimized two-step hybrid block method for solving general second order initial-value problems. *Numer Algo*. 2016;72:1089-1102.
16. Rufai MA, Ramos H. A variable step-size fourth derivative hybrid block strategy for integrating third-order IVPs, with applications. *Int J Comput Math*. 2022;99(2):292-308.
17. Rufai MA, Ramos H. Solving third-order Lane-Emden-Fowler equations using a variable step-size formulation of a pair of block methods. *J Comput Appl Math*. 2023;420:114776.
18. Ramos H, Rufai MA. Third derivative modification of k-step block Falkner methods for the numerical solution of second order initial-value problems. *J Appl Math Comput*. 2018;333:231-245.
19. Ramos H, Rufai MA. An adaptive one-point second-derivative Lobatto-type method for solving efficiently differential systems. *Int J Comput Math*. 2022;99(8):1687-1705.
20. Ramos H, Rufai MA. An adaptive pair of one-step hybrid block Nyström methods for singular initial-value problems of Lane-Emden-Fowler type. *Math Comput Simul*. 2022;193:497-508.
21. Ramos H, Rufai MA. Two-step hybrid block method with fourth derivatives for solving third-order boundary value problems. *J Comput Appl Math*. 2022;404:113419.
22. Amodio P, Brugnano L. Parallel implementation of block boundary value methods for ODEs. *J Comput Appl Math*. 1997;78(2):197-211.

23. Rufai MA. An efficient third-derivative hybrid block method for the solution of second-order BVPs. *Mathematics*. 2022;10(19):3692.
24. Hairer E, Wanner G. A theory for Nyström methods. *Numer Math*. 1975;25(4):383-400.
25. Van der Houwen PJ, Sommeijer BP, Nguyen HC. Stability of collocation-based Runge-Kutta-Nyström methods. *BIT*. 1991;31:469-481.
26. Hairer E, Nørsett SP, Wanner G. *Solving Ordinary Differential Equations, I. Nonstiff Problems, second revised edition*. Berlin: Springer-Verlag; 1987.
27. Rufai MA, Ramos H. Numerical solution of second-order singular problems arising in astrophysics by combining a pair of one-step hybrid block Nyström methods. *Astrophys Space Sci*. 2020;365:96.
28. Atkinson K. *Elementary Numerical Analysis*. 2d edition. New York: Wiley Sons John; 1993.
29. Shampine LF, Gordon MK. *Computer Solutions of Ordinary differential Equations: The Initial Value Problem*. Freeman, San Francisco, CA 1975.
30. Iavernaro F, Mazzia F. A fourth order symplectic and conjugate-symplectic extension of the midpoint and trapezoidal methods. *Mathematics*. 2021;9(10):1103.
31. Mazzia F, Sestini A. On a class of conjugate symplectic Hermite-Obreshkov one-step methods with continuous spline extension. *Axioms*. 2018;7(3):58.
32. Stoer J, Bulirsch R. *Introduction to Numerical Analysis*: Springer; 2002.
33. Vigo-Aguiar J, Ramos H. Variable stepsize implementation of multistep methods for $y'' = f(x, y, y')$. *J Comput Appl Math*. 2006;192:114-131.
34. Amodio P, Settanni G. High order finite difference schemes for the solution of second order initial value problems. *JAIAM J Numer Anal Ind Appl Math*. 2010;5:3-16.
35. Amodio P, Budd CJ, Koch O, Settanni G, Weinmüller EB. Asymptotical computations for a model of flow in saturated porous media. *Appl Math Comput*. 2014;237:155-167.
36. Butcher JC. *Numerical Methods for Ordinary Differential Equations*: John Wiley and Sons; 2008.
37. Dormand JR, El-Mikkawy MEA, Prince PJ. Families of Runge-Kutta-Nyström formulae. *IMA J Numer Anal*. 1987;7:235-250.
38. Mazzia F, Iavernaro F. Test set for initial value problems solvers. Department of Mathematics University of Bari; 2003.
39. Amodio P, Iavernaro F. Symmetric boundary value methods for second order initial and boundary value problems. *MedJM*. 2006;3:383-398.

How to cite this article: Rufai MA, Mazzia F, Ramos H. An adaptive optimized Nyström method for second-order IVPs. *Math Meth Appl Sci*. 2022;1-14. doi:10.1002/mma.8983